# Impact of AlN-aperture on Optical and Electrical Properties on Nitride VCSEL

P. Śpiewak, A. K. Sokół, M. Wasiak and R. P. Sarzała
Photonics Group, Institute of Physics, Lodz University of Technology
Wólczańska 219
90-924 Łódź, Poland, robert.sarzala@p.lodz.pl

***Abstract*–We report a numerical analysis of nitride VCSELs with ITO (indium-tin-oxide) current spreading layers and AlN apertures. The results show that the position and thickness of the AlN aperture significantly influences optical and electrical properties of the analyzed structure and that the influence depends on the thickness, location and diameter of this aperture.**

## I. Introduction

The success of GaAs-based VCSELs (vertical-cavity surface-emitting lasers) showed a big potential of this type of semiconductor lasers. Nitride VCSELs are still at an early stage of development and there is a need to search for new solutions. The main problems of nitride VCSELs are: difficulties in fabricating DBR (distributed Bragg reflectors) mirrors, and non-uniform current distribution in the active region. In arsenide VCSELs, oxide electrical and optical apertures are widely used. In nitride materials fabrication of oxidation is not possible. Currently, in order to concentrate the current near the center of a nitride VCSEL, semi-transparent ITO contacts or tunnel junctions are used [1]. However, recently group from Taiwan proposed a laser with AlN-buried structure (analogous to oxide-apertures in arsenide lasers) [2]. In this paper, we analyzed impact of the position and thickness of such an AlN-aperture on threshold parameters and mode profiles in nitride VCSELs with an ITO contact.

## II. The Laser Structure

The modeled laser is based on a device fabricated at University Chiao Tung in Taiwan [2, 3]. Fig. 1 presents a schematic diagram of the analyzed structure. This structure has a dielectric top DBR mirror and a native (made of nitride materials) bottom DBR mirror. In the original structure, optical confinement is provided by a 0.5-μm-wide gold ring of the inner radius $r_{Au}$. In this paper, we analyze different types of structure: structures similar to the original structure, and structures with additional AlN layers defining different apertures. We consider different locations and thicknesses of these apertures (see Fig. 1 and Fig. 2). In two cases the AlN aperture is located near a node of the standing wave, in the third case the AlN aperture is at an anti-node. More details of the model and the parameters used are described in [4]. In the simulations presented in this paper we assume that all the structures are detuned, which means that the emission wavelength (determined by the thickness of the resonator) is bigger than the wavelength of the maximal gain in the active region.

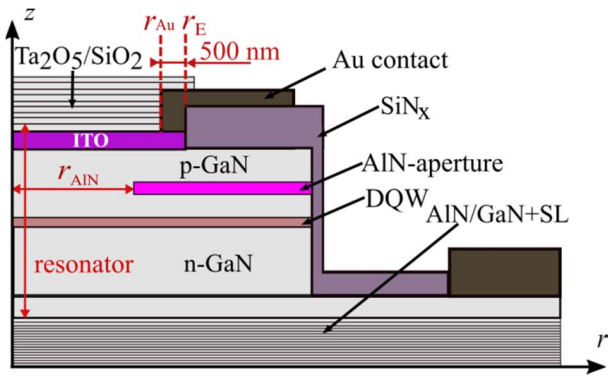


Fig. 1. Schematic diagram of the structure of the modelled VCSEL, $r_{Au}$ – radius of the gold ring, $r_E$ – radius of the electrical aperture, $r_{AlN}$ – radius of the AlN aperture, SL – superlattices.

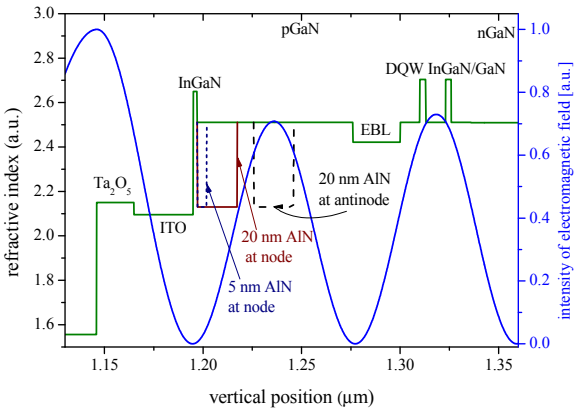


Fig. 2. Distribution of the optical field intensity and index of refraction profiles near the active region, ITO – indium-tin-oxide layer, EBL – AlGaN electron blocking layer.

## III. Results

We modelled the RT (room temperature), CW (continuous-wave) operation of the detuned structure with three different AlN-aperture confinement schemes. Fig. 3 shows threshold currents as functions of the radius of the AlN-aperture. The structures with the AlN-apertures at the antinode have the lower threshold currents than the structures with the AlN-apertures at the node. If the AlN layer is located at an

978-1-4673-8603-6/16/$31.00 ©2016 IEEE

antinode, it strongly confines the modes. In contrast, when the AlN-aperture is placed at node, high order modes are not confined by a thin (5 nm) AlN layer or weakly confined by a 20-nm-thick AlN layer (Fig.4). If a high order mode is not confined within the AlN-aperture, it penetrates the gold ring which generates significant optical losses. Therefore structures with the AlN-apertures at the a node operate at low-order (longer-wavelength) modes which have lower material gain (because the structure is detuned), so their threshold currents are higher.

If the AlN aperture is equal to the gold ring aperture (9 µm diameter) or bigger, the impact of the AlN layer disappears, because the modes are strongly confined by the gold ring, and the optical field does not interacts with AlN. For this reason all the curves in Fig. 3 overlap for $r_{AlN} \geq 4.5$ µm.

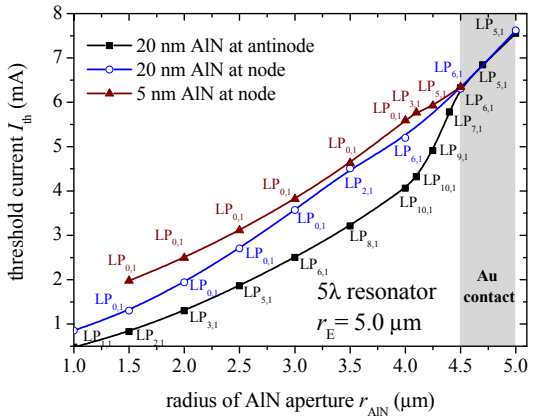


Fig. 3. Threshold current as a function of the radius of the AlN-aperture for laser with 5λ resonator and $r_E$ = 5 µm ITO layer radius. Threshold transverse modes are indicated.

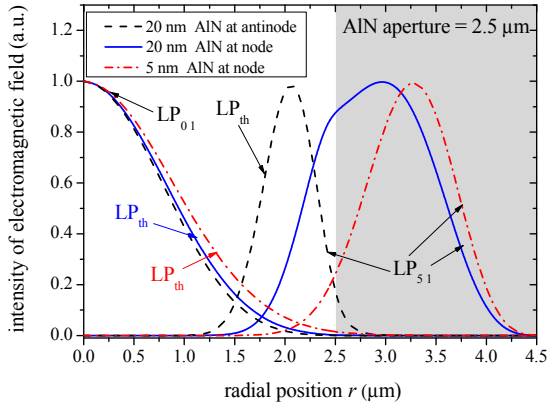


Fig. 4. Intensity profiles for the $LP_{01}$ and $LP_{51}$ modes at the laser's threshold for various positions and thicknesses of the AlN aperture. $LP_{th}$ indicates the lasing mode for the each case.

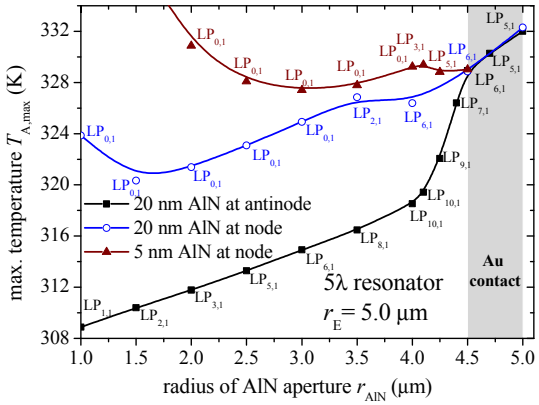


Fig. 5. Maximum temperature in the active area at threshold as a function of the radius of the AlN aperture. Threshold transverse modes are indicated. The ambient temperature is 300 K.

By positioning of the AlN aperture near the node of the standing wave we can make the laser to operate on the fundamental mode. However there is a difference in the threshold current and temperature (see Fig. 3 and 5) between the structures with the thin (5 nm) and thick (20 nm) AlN layer. In the second case, the fundamental mode wider (see Fig. 4) and suffers higher losses in the active region in the area outside the aperture which is not excited by the current. Because of this, the threshold currents and temperatures are highest in the structures with the thin AlN layer located at the node of the standing wave. For example, for the 2.5-µm radius aperture, the electrical input power for the 5-nm thick AlN layer positioned at the wave node is over two times higher than for the 20-nm thick AlN layer at the wave antinode. This results also in the twofold temperature increase which can be seen in Fig. 5.

## ACKNOWLEDGMENT

This work was partially supported by the National Science Centre, Poland, Project 2014/13/B/ST7/00633.

## REFERENCES

[1] J. T. Leonard, E. C. Young, B. P. Yonkee, D. A. Cohen, C. Shen, T. Margalith, T. K. Ng, S. P. DenBaars, B. S. Ooi, J. S. Speck, S. Nakamura, "Comparison of nonpolar III-nitride vertical-cavity surface-emitting lasers with tunnel junction and ITO intracavity contacts" *Proc. SPIE* 9748, Gallium Nitride Materials and Devices XI, 97481B, 2016

[2] Y. Y. Lai, S. C. Huang, T.-L. Ho, T.-C. Lu,1, and S.-C. Wang1, "Numerical analysis on current and optical confinement of III-nitride vertical cavity surface-emitting lasers", *Optics Express 9789,* vol. 22, no. 8, 2014.

[3] T.-C. Lu, S.-W. Chen, T.-T. Wu, P.-M. Tu, C.-K. Chen, C.-H. Chen, Z.-Y. Li, H.-C. Kuo, and S.-C. Wang, "Continuous wave operation of current injected GaN vertical cavity surface emitting lasers at room temperature", *Appl. Phys. Lett.*, vol. 97, no. 7, pp. 071114, 2010.

[4] M. Marciniak, P. Śpiewak, M. Więckowska, and R. P. Sarzała, *Przegląd Elektrotechniczny* 1, 127 (2015).